

Alma Mater Studiorum Università di Bologna
Archivio istituzionale della ricerca

Boosting Direct X-Ray Detection in Organic Thin Films by Small Molecules Tailoring

This is the final peer-reviewed author's accepted manuscript (postprint) of the following publication:

Published Version:

Ciavatti, A., Basiricò, L., Fratelli, I., Lai, S., Cosseddu, P., Bonfiglio, A., et al. (2019). Boosting Direct X-Ray Detection in Organic Thin Films by Small Molecules Tailoring. *ADVANCED FUNCTIONAL MATERIALS*, 29(21), 1-8 [10.1002/adfm.201806119].

Availability:

This version is available at: <https://hdl.handle.net/11585/667346> since: 2019-02-18

Published:

DOI: <http://doi.org/10.1002/adfm.201806119>

Terms of use:

Some rights reserved. The terms and conditions for the reuse of this version of the manuscript are specified in the publishing policy. For all terms of use and more information see the publisher's website.

This item was downloaded from IRIS Università di Bologna (<https://cris.unibo.it/>).
When citing, please refer to the published version.

(Article begins on next page)

This is the final peer-reviewed accepted manuscript of:

Andrea Ciavatti, Laura Basiricò, Ilaria Fratelli, Stefano Lai, Piero Cosseddu, Annalisa Bonfiglio, John E. Anthony, Beatrice Fraboni, *Boosting Direct X-Ray Detection in Organic Thin Films by Small Molecules Tailoring*, in ADVANCED FUNCTIONAL MATERIALS, 2019, 29, 1806119.

The final published version is available at: <https://doi.org/10.1002/adfm.201806119>

Rights / License:

The terms and conditions for the reuse of this version of the manuscript are specified in the publishing policy. For all terms of use and more information see the publisher's website.

This item was downloaded from IRIS Università di Bologna (<https://cris.unibo.it/>)

When citing, please refer to the published version.

DOI: 10.1002/ ((please add manuscript number))

Article type: Full paper

Boosting direct X-ray detection in organic thin films by small molecules tailoring

Andrea Ciavatti, Laura Basiricò, Ilaria Fratelli, Stefano Lai, Piero Cosseddu, Annalisa Bonfiglio, John E. Anthony and Beatrice Fraboni**

Dr. A. Ciavatti, Dr. L. Basiricò, I. Fratelli and Prof. B. Fraboni

Department of Physics and Astronomy, University of Bologna, Viale Bertini Pichat 6/2, Bologna 40127, Italy

E-mail: andrea.ciavatti2@unibo.it, beatrice.fraboni@unibo.it

Prof. J. E. Anthony

Center for Applied Energy Research, University of Kentucky, Lexington, Kentucky 40511, USA

Dr. S. Lai, Prof. P. Cosseddu, Prof. A. Bonfiglio

Department of Electrical and Electronic Engineering, University of Cagliari, Piazza D'Armi, Cagliari 09123, Italy

This is the author manuscript accepted for publication and has undergone full peer review but has not been through the copyediting, typesetting, pagination and proofreading process, which may lead to differences between this version and the [Version of Record](#). Please cite this article as [doi: 10.1002/adfm.201806119](#).

This article is protected by copyright. All rights reserved.

Keywords: organic x-ray detectors, thin film transistors, tips-pentacene, tipge-pentacene

The attention on the application of organic electronics for the detection of ionizing radiation is rapidly growing among the international scientific community, due to the great potential of the organic technology to enable large-area conformable sensor panels. However, high-energy photon absorption is challenging as organic materials are constituted of atoms with low atomic numbers. Here it is reported how, by synthesizing new solution-processable organic molecules derived from 6,13-bis(triisopropylsilyl)ethynylpentacene (TIPS-pentacene) and 2,8-Difluoro-5,11-bis(triethylsilyl)ethynylanthradithiophene (diF-TES-ADT), with Ge-substitution in place of the Si atoms to increase the material atomic number, it is possible to boost the X-ray detection performance of organic thin films on flexible plastic substrates. TIPGe-pentacene based flexible OTFTs show high electrical performance with higher mobility ($0.4 \text{ cm}^2 \text{ V}^{-1} \text{ s}^{-1}$) and enhanced X-ray sensitivity, up to $9.0 \times 10^5 \text{ } \mu\text{C Gy}^{-1} \text{ cm}^{-3}$, with respect to TIPS-pentacene based detectors. Moreover, similar results are obtained for diF-TEG-ADT devices, confirming that the proposed strategy, i.e. increasing the atomic number of organic molecules by chemical tailoring to improve X-ray sensitivity, can be generalized to organic thin film detectors, combining high X-ray absorption, mechanical flexibility and large area processing.

1. Introduction

The detection of ionizing radiation is an increasingly important task in a great number of industrially and socially relevant activities, such as medical diagnostics and therapy, cultural heritage, citizen and airport security, defence, environmental monitoring, non-destructive industrial testing, and wearable personal dosimetry^[1]. In particular, large area, thin, flexible sensors are needed to detect ionizing radiation impinging on complex geometrical structures in real-time and at affordable costs. Unfortunately, current technologies cannot deliver all these features in one single device^[2]. Concerning direct detectors, they are typically solid-state devices based on inorganic materials (silicon, cadmium telluride, amorphous selenium, silicon carbide, diamond, and others), which indeed offer excellent detecting performance, but are rigid, heavy, power-consuming, toxic in some cases and only allow a small active detection area^[3,4]. The quest for flexibility, conformability, low cost, low-power consumption and portability (i.e. low weight and battery supply operation), will require new materials and device architectures.

Organic materials have recently attracted major attention because they demonstrated, in the case of other electronic/optoelectronic devices (e.g. transistors^[5,6], organic solar cells^[7,8]), room temperature operation, low environmental impact, low fabrication costs and the possibility of fabricating transparent and flexible devices, allowing unprecedented and integrated device functions and architectures. As ionizing radiation detectors, fully organic direct detectors based on organic semiconducting thin crystals and polymers have demonstrated promising active sensing properties, despite their lower carrier mobility and low ionizing radiation absorption coefficient with respect to inorganic semiconductors^[9–11]. In particular, solution-processed flexible direct radiation detectors based on organic thin film transistors (OTFTs) with a 100nm-thick micro-crystalline (e.g. TIPS-pentacene) active layer have been recently reported to outperform all the polymeric devices

sensitivity, operating at room temperature and at very low bias voltages ($<5V$), thanks to a photoconductive gain mechanism^[12,13].

However, in such devices high-energy photon absorption is challenging as organic materials are constituted of atoms with low Z atomic numbers. The blending into the organic matrix of high- Z nanoparticles^[14,15], carbon nanotubes^[16] and inorganic micrometer-sized scintillating particles^[17] has been explored as a possible solution. However, although improvement in the detecting performance has been shown, for all of the above solutions, the presence of even small fractions of the “dopant” (i.e. nanoparticles, carbon nanotubes or scintillating particles) strongly degrade the electrical performance and the stability of the organic film. Moreover, the employment of thick films^[18] or bulky single crystals^[10,19] to increase the absorption, results in an increase of the operating voltage and limits the bendability of the device, thus sacrificing the potential advantages.

More recently, hybrid lead-halide perovskites have broken into the scene as alternative candidates to organic materials, as they combine excellent semiconducting properties like high charge carrier mobility and long diffusion length, with high- Z elements (such as Pb) intrinsically incorporated into the ionic crystal structure^[20,21]. Despite the evidence of record sensitivity values, their instability due to strong reactivity in air and the lack of comprehension on ionic current mechanism, up to now restrict their employment in real life applications and limit their industrial scalability.

We propose here an alternative approach to increase radiation capture cross-section that takes advantage of the “tunability” of organic materials by addition of high- Z atoms into the basic molecular structure. These intrinsically improve the ionizing radiation absorption while maintaining

the low-cost, the solution-processability and the mechanical flexibility peculiar to organic materials, as well as the high structural quality and charge transport properties of the deposited thin films.

Here we report how, by synthesizing new solution-processable organic molecules derived from 6,13-bis(triisopropylsilyl)ethynyl)pentacene (TIPS-pentacene) and 2,8-Difluoro-5,11-bis(triethylsilyl)ethynyl)anthradithiophene (diF-TES-ADT), with Ge-substitution in place of the Si atoms to increase the material atomic number, we boosted the X-ray detection performance of organic thin films. X-ray detectors based on such organic thin films show an X-ray mass absorption coefficient ten times higher than their silicon counterparts, better charge transport properties, an X-ray sensitivity per unit area comparable with amorphous selenium and a good crystalline morphology.

2. Consideration on Photoconductive Gain

The high X-ray sensitivities reported for organic thin films pushed the performance of organic flexible detectors closer to the one of inorganic detectors thanks to a photoconductive gain mechanism, as mentioned above. Nonetheless, a further step in their radiation detection sensitivity is necessary to make them competitive against current technologies and to fulfil the required market specifications. In the following, we recall the principles of the photoconductive gain process, in order to discuss how to possibly increase the electrical signal output and the X-ray sensitivity in organic thin film X-ray detectors. The X-ray photocurrent is given by $\Delta I = G I_{CC}$, where $G = \tau_r / \tau_t$ is the gain factor, τ_r the free carrier lifetime and $\tau_t = L^2 / \mu V$ the carrier transit time (see reference ^[12] for details on the model). I_{CC} is the photocurrent generated by primary collection of the charges generated by the direct X-ray absorption in the active layer. I_{CC} is proportional to the photon

absorption rate, which is very low for organic thin films (attenuated fraction of 0.0015% for 150 nm thick film of TIPS-pentacene). On the other hand, the gain factor can be maximized by increasing the free carrier lifetime τ_r and by reducing the carrier transit time τ_t . The transit time reduces if the carrier mobility μ increases. Shortening the channel length L or increasing the bias voltage V reduces τ_t , but, at the same time, results in a large increase of the dark current I_0 and in the electrical instability of the device. The analytical expression of τ_r is complex, however, considering its most used empirical description for organic thin films; it is related to the charge carrier density flowing into the device. To summarize, three major approaches can be considered to enhance the X-ray sensitivity of organic thin film detectors: i) increase the radiation absorption, maximizing the primary generated charge carriers; ii) increase the charge carrier mobility, reducing τ_t and improving the charge collection efficiency; iii) increasing the charge carrier density to maximize τ_r and thus the gain factor.

3. Results

Bearing in mind the above considerations, we synthesized bis(triisopropylgermylethynyl) pentacene (TIPGe-pentacene, hereafter TIPGe), where Ge atoms substitute Si atoms in the TIPS-pentacene (hereafter TIPS) molecule (**Figure 1a**)^[22]. Thanks to the much higher Ge atomic number ($Z = 32$) than the one of Si atoms ($Z = 14$) the X-ray attenuated fraction of TIPGe is intrinsically much higher than the TIPS molecule (**Figure 1b**), and the attenuation length at an X-ray energy of 17keV, is ten times shorter (7.8 mm for TIPS and 0.6 mm for TIPGe). Moreover, the substitution of Ge for Si led to a new material with similar solubility and processing parameters as TIPS. Actually, TIPGe keeps

many of the desirable features of TIPS, like solution processability, good morphology, nice film crystallization and very good electrical properties in the thin film shape.

TIPGe thin films were grown by drop-casting onto interdigitated gold electrodes on flexible plastic substrate (details in experimental section). Good crystallization and uniform polycrystalline films were obtained, enabling the efficient flow of electrical current through the fingers of the electrodes. Optical and AFM images show needle-like crystals, hundreds of micrometer-long and 200 nm thick (**Figure 1c** and **Figure S1**). The coverage of the active area strongly depends on the deposition conditions and vary from 40% to 75% of the full relevant surface. The X-ray attenuated fraction at the considered energy of 17keV ($K\alpha$ peak of Mo) in a 200nm thick film of TIPGe is 0.034%, a value that may seem low but is actually twenty times higher than the one for equivalent TIPS drop-cast thin films (**Figure S2**). UV-Vis photocurrent spectroscopy investigation confirms the good optoelectronic properties of the film and its quality. A high and stable photocurrent signal with a smooth spectrum presenting evident vibronic modes was obtained, as expected for such devices^[23,24] (**Figure 1d**). The forbidden energy gap has been extracted from the Tauc formula^[25], since the UV-Vis photocurrent signal is well approximated by the absorption spectrum in low absorption condition as at the rising edge of the gap^[26]. The measured energy gap for TIPGe is (1.60 ± 0.03) eV, slightly larger than the one of TIPS, (1.56 ± 0.09) eV (**Figure S3**).

Direct X-ray detector devices have been realized by depositing TIPGe films onto bottom gate bottom contact low-voltage Organic Thin Film Transistors (OTFTs) on flexible PET substrates (**Figure 2a** and experimental section). This structure was used previously to obtain TIPS thin film devices with the highest X-ray sensitivity reported^[13], thus constituting an optimal benchmark for the characterization of TIPGe detecting performance. Moreover, the OTFT architecture will allow us to extract the mobility values and the electronic performance of TIPGe-devices which has never before

been subjected before to studies in transistor configurations^[22]. We fabricated OTFTs from solutions of TIPGe at a concentration of 0.5wt.% in toluene or in chlorobenzene solvent, and we monitored the solvent effects on the mobility, the threshold voltage and the on/off current ratio. We further investigated the impact of using interdigitated (the geometry used for detectors to maximize the sensitivity) or linear source-drain electrodes. Statistical results over 45 devices are reported in the Supplementary Information Section (**Figure S4**). In general, very good p-type transistors were obtained. The typical electrical behavior of TIPGe OTFT devices fabricated with the optimized recipe is reported in **Figure 2b,c**. The output I_{DS} - V_{DS} characteristics present excellent field effect and saturation in the drain current (**Figure 2b**). No hysteresis is visible and low contact resistance is present, proving the good quality of the deposited films and the efficient charge injection at the electrodes. In addition, the transfer I_{DS} - V_{GS} characteristics show very low threshold voltage ($< -0.2V$), low leakage current ($< 10^{-9}A$) and good on/off ratio (10^2 - 10^5) (**Figure 2c**). The average mobility values for devices with chlorobenzene solvent is $(0.28 \pm 0.11) \text{ cm}^2 \text{ V}^{-1} \text{ s}^{-1}$, while the highest measured value was $0.40 \text{ cm}^2 \text{ V}^{-1} \text{ s}^{-1}$. These mobility values are not the highest reported in the literature for organic thin films, as we fabricated our devices by solution on flexible plastic substrates. Indeed, it is noteworthy that the value is close to the highest reported one for solution-processable flexible OTFTs^[27] and more than one order of magnitude better than for TIPS based OTFTs, $(0.018 \pm 0.010) \text{ cm}^2 \text{ V}^{-1} \text{ s}^{-1}$, fabricated on exactly the same device architecture (**Figure 2d**). To evaluate the mechanical flexibility the devices have been stressed by incrementally reducing the bending radius and thus increasing the strain on the film. The current variation is small up to strain of 1% (**Figure S5a**). The transfer characteristic returns to the starting points when the samples are restored in the initial flat state at the end of the procedure (**Figure S5b**), meaning that no permanent damages are induced in

40 minutes of bending (the time of the full process). The results are in line with the mechanical stress studies on similar OTFTs architectures based on TIPS^[28,29].

Low-voltage OTFTs based on TIPGe are therefore suitable for high sensitivity direct X-ray detectors compared to TIPS, since beside the higher X-ray absorption, TIPGe also exhibits higher charge carrier mobility. The typical X-ray photocurrent response of TIPGe based OTFT detectors, working in saturation regime ($V_{DS} = -3V$, $V_{GS} = -2V$), is reported in **Figure 3a**. The signal follows the typical dynamic where the photoconductive gain process dominates: it quickly increases immediately after switching on the radiation and reaches saturation after a few tens of seconds. The response is repeatable and nicely scales with the dose rate. In particular, the signal amplitude in I_{DS} , which is on the order of hundreds of nanoamperes, increases linearly with the dose rate, as expected in photoconductive gain model for “short” exposure (i.e. when the exposure time is lower than the time needed to reach saturation) (**Figure 3b**). The X-ray induced gate current is limited to 20 pA, negligible in respect to X-ray photocurrent at I_{DS} . The mean sensitivity (averaged over 15 samples) is $(3080 \pm 20) \text{ nC Gy}^{-1}$ ($(6.2 \pm 0.1) \times 10^5 \mu\text{C Gy}^{-1} \text{ cm}^{-3}$) (**Figure 3e**), with top recorded value of $(4460 \pm 50) \text{ nC Gy}^{-1}$ ($(9.0 \pm 0.1) \times 10^5 \mu\text{C Gy}^{-1} \text{ cm}^{-3}$) (**Figure S7**). The direct comparison with TIPS thin film detectors fabricated on the same flexible substrate^[13] confirms the better performance of TIPGe. In fact, the average sensitivity of TIPGe thin film detectors is three times higher than for TIPS-based devices (**Figure 3b, c**). **Figure 3e** summarizes the main features and the sensitivity values of TIPS and TIPGe OTFTs X-ray detectors. Indeed, the improvement of X-ray sensitivity of TIPGe-based detectors is potentially even higher. In fact, the average detector active area coverage of TIPS crystallites is about 76% with small variation between the samples, while the variation of percentage of full coverage in TIPGe-based devices is relevant, in the range 40-75%. If we calculate the potential sensitivity, i.e. the sensitivity normalized for the actual coverage as if the full area is covered, we

obtain $3.4 \times 10^5 \mu\text{C Gy}^{-1} \text{cm}^{-3}$ for TIPS devices, and $21 \times 10^5 \mu\text{C Gy}^{-1} \text{cm}^{-3}$ for TIPGe ones (with an area coverage is only 43%, see **Figure S7a**). It is noteworthy that the average sensitivity per unit volume of TIPGe detectors is the highest reported among solid state X-ray detectors^[15]. Moreover, the corresponding sensitivity per unit area, equal to $12.3 \mu\text{C Gy}^{-1} \text{cm}^{-2}$, is competitive with some state-of-the-art inorganic materials currently used to fabricate large area detectors (amorphous selenium has typical values of $25 \mu\text{C Gy}^{-1} \text{cm}^{-2}$)^[30]. This is a fundamental milestone for organic ionizing radiation detectors, making their performance comparable and competitive with commercial devices, while maintaining the peculiarities of organic thin films, i.e. the low-cost, the low voltage operation and the mechanical flexibility.

We have also considered and assessed the minimum detectable dose by TIPGe detectors. **Figure 3c and 3d** report the photocurrent response of TIPGe detectors as function of time and of dose rate, respectively, in linear region ($V_{DS} = -0.5\text{V}$) at low exposure doses, down to a dose rate of $6.4 \mu\text{Gy s}^{-1}$. Remarkably, the detectors show a linear response to X-rays over four orders of magnitude in the dose rate range. If we estimate the lowest detectable dose rate (defined as three times the detector noise) from the slope of the linear fit of **Figure 3d**, it results equal to $1.66 \mu\text{Gy s}^{-1}$. In addition, we have measured the smallest total dose detectable over an X-ray exposition of 1 s and we could reliably detect down to $12 \mu\text{Gy}$ have been detected (**Figure S6**). These values are the lowest reported for organic direct X-ray detectors, and are below the threshold of regular medical diagnostic (dose rate about $5.5 \mu\text{Gy s}^{-1}$)^[31,32]. Noteworthy, also the minimum total dose is close to the values reported for high performing thick perovskites X-ray direct detectors as wavers^[21] ($10 \mu\text{Gy}$) or single crystals^[33] ($0.5 \mu\text{Gy}$).

At the considered energy range (17keV) the primary X-ray/organic materials interaction is dominated by photoelectric effect (**Figure S8a**). Thus, the role of metal electrodes cannot be

ignored, as a non-negligible contribution has already been reported^[13,19]. The impact of the layers of the transistor structure (Al gate, Al₂O₃/Parylene dielectric, Au source/drain electrodes) on the X-ray photoresponse signal amplitude has been evaluated by measuring the X-ray response of a blank device, i.e. the OTFT structure of **Figure 2a**, without the active organic layer (**Figure S8b**). The contribution to the drain current is of 315 pA at dose rate of 56 mGy/s and driving voltage $V_{DS}=-3V$, $V_{GS}=-2V$ and the one to the gate current is of 20pA. The value is negligible (much less than 1%) in comparison with hundreds of nano-amperes of the total signal amplitude.

Commenting the above results, the generated photocurrent is the product of the gain factor G and the primary collected charges I_{CC} : the gain factor G rises proportionally with the improvement of mobility, while I_{CC} increases with the improvement of X-ray absorption. The combination of these two factors would results in a much higher TIPGe sensitivity compared to TIPS devices. The values we have obtained can be only partially explained by the difference of area coverage between TIPS and TIPGe. Thus, we believe the performance of TIPGe detectors could be further improved by investigating the effects that may affect the detection process, like the energetic barrier at Au/organic interfaces that limit injection, or the distribution and recombination time of electrically active charge traps.

So far, we have demonstrated that the idea of chemical tailoring of known organic molecules (TIPS) to synthesize a new molecule with high-Z atoms intrinsically bonded into the basic molecule (TIPGe) is effective. We would like to generalize the idea. Thus, we have fabricated spin-coated OTFTs employing the fluorinated molecule diF-TES-ADT (**Figure 4a**) and its derivative with germanium in place of silicon atoms, 5,11-bis(triethylgermylethynyl)anthradithiophene (diF-TEG-ADT) (**Figure 4b**). The crystallization of 1.2wt.% of diF-TES-ADT in chlorobenzene solution spin-coated on plastic substrate is very good: large and thick (thickness 120 nm) crystals are observed in

AFM maps (**Figure 4a**). For diF-TEG-ADT material, instead, small needle-like crystallites (thickness 90 nm) have been observed (**Figure 4b**). Despite the different crystallites dimension, their total area coverage is comparable (87% for diF-TES-ADT and 88% for diF-TEG-ADT). The X-ray attenuated fraction is equal to 0.0031% for diF-TES-ADT and 0.015% for diF-TEG-ADT (**Figure S2**). For both materials good field effect mobility in low voltage transistor devices have been obtained (**Figure S9**). In spite of the crystal dimensions, diF-TEG-ADT devices show on average a better mobility compared to diF-TES-ADT ones^[34]. However, we choose to compare as X-ray detectors only devices with comparable mobility values, in order to explicitly exclude its effects on X-ray sensitivity. **Figure 4c** reports the X-ray photocurrent vs. dose rate of diF-TES-ADT and diF-TEG-ADT transistors, with mobility of $(5.2 \pm 0.3) \times 10^{-2} \text{ cm}^2 \text{ V}^{-1} \text{ s}^{-1}$ and $(6.9 \pm 0.4) \times 10^{-2} \text{ cm}^2 \text{ V}^{-1} \text{ s}^{-1}$, respectively. The extracted sensitivity of diF-TEG-ADT-based detectors (3400 ± 400) nC mGy⁻¹ cm⁻³ is forty times higher than the one calculated for diF-TES-ADT devices (**Figure 4d**). This crosscheck test therefore confirms the effectiveness of our proposed strategy, i.e. increasing the atomic number of organic molecules by chemical tailoring, that successfully leads to the improvement in X-ray sensitivity of organic thin film detectors. This result represents an important step forward for the exploitation of organic detectors as commercially competitive flexible devices for X-ray detection systems.

Finally, with the aim of maximizing the sensitivity to ionizing radiation, we also studied the role of the organic molecule concentration, depositing films of TIPGe in different concentration, spanning from 0.5wt.% to 4wt.% in toluene solution, by both dropcast or spincoast deposition methods. As expected, the thickness of the crystals and the coverage of the electrodes area increase with the rising TIPGe concentration. In particular optical microscope images and AFM maps analyses show 200nm thick crystals and coverage of 72% for 0.5wt.% solution (**Figure 5a**), 300nm thick crystals and coverage of 77% for 1wt.% solution (**Figure 5b**) and 1μm thick crystals and coverage of

91% for 4wt.% solution (**Figure 5c**). As a result, not only the film morphology, but also the OTFT mobility and the X-ray sensitivity are strongly affected by the solution concentration. The mobility decreases by more than four times from 0.5wt.% to 4wt.%; similarly, the X-ray sensitivity decreases by one order of magnitude (**Figure 5d**). The latter results indicate that the thinnest film obtained with the less concentrated solution is the best performing in term of both mobility and X-ray sensitivity. In addition, it highlights an important concept: although thicker films absorb a larger amount of X-ray photons, the degradation of the transport properties inhibits the photoconductive gain mechanism, thus reducing the total detector sensitivity.

4. Conclusion

In this work we demonstrate a novel approach to increase the X-ray detection performance of organic thin film detectors. With the aim to improve the X-ray absorption of the organic detectors we synthesize a new solution-processable organic small molecule derived from TIPS-pentacene with Ge-substitution in place of the Si atoms, namely TIPGe, with an improvement of the material mass absorption coefficient by a factor of 10. Moreover, TIPGe shows higher FET charge carrier mobility, i.e. $0.28 \text{ cm}^2 \text{ V}^{-1} \text{ s}^{-1}$ vs. $0.018 \text{ cm}^2 \text{ V}^{-1} \text{ s}^{-1}$ of TIPS-pentacene. The combination of higher X-ray absorption and improved mobility leads to five times higher sensitivity of TIPGe based OTFT X-ray detectors compared to TIPS-pentacene, reaching $9.0 \times 10^5 \text{ } \mu\text{C Gy}^{-1} \text{ cm}^{-3}$, the record value for organic/hybrid X-ray direct detectors reported in literature so far. In order to assess the general aspect of the proposed strategy, the experiments have been repeated by comparing the X-ray detection performances of diF-TES-ADT and diF-TEG-ADT based OTFTs, finding that also in this case the Ge-containing molecule shows improved X-ray sensitivity. This latter result thus confirms how

the small molecules tailored with high-Z elements represents a winning general strategy to increase X-ray detection performance, maintaining good transport and collection properties, for thin film based organic direct ionizing radiation detectors.

5. Experimental Section

Synthesis of Organic Molecules: TIPS-pentacene^[35], TIPGe-pentacene^[22], diF-TES-ADT^[36], and diF-TEG-ADT^[34] were prepared according to literature procedures.

Device Fabrication: Devices are entirely fabricated over 175 μm thick, biaxially oriented polyethylene terephthalate (PET) substrates. Low-voltage OTFTs are fabricated using the procedure reported by Cosseddu *et al.*^[37]. Both linear ($W/L = 3000 \mu\text{m}/45 \mu\text{m} = 66.7$) and interdigitated source-drain electrodes geometry ($W/L = 50\,000 \mu\text{m}/45 \mu\text{m} = 1223$) have been used in electrical characterization. The interdigitated geometry was chosen for detectors.

The semiconductor layer has been deposited by the following procedures:

- TIPGe: 0.5wt.%, 1wt% and 4wt% in toluene or chlorobenzene TIPGe solution is deposited on the whole structure by drop cast. During the deposition of the organic solution, the substrate is kept at 60°C, after the deposition the devices are annealed at 80°C for 1 h.
- diF-TES-ADT and diF-TEG-ADT: 1.2wt% in chlorobenzene are spin cast at 1000 rpm for 60 s with an acceleration time of 1 s. After the deposition, the samples are put under vacuum ($\approx 0.1 \text{ mbar}$) for 24 hours in order to remove the solvent.

Electrical Characterization: Electrical characterization are performed with a dual channel Keithley 2614B SourceMeter, using a triaxial cables (that ensure low noise down to 10^{-13} A and low parasitic capacitance) and custom made Labview software. All measurements are carried out keeping the device in dark in a metal Faraday cage to reduce electrical noise and avoid light-induced photogeneration in the organic semiconductor.

AFM measurements: AFM measurements are performed on a Park NX10 system using PPP-NCHR tips (Nanosensors) in non-contact mode and applying adaptive scan-rate to slow down scan speed at crystallite borders.

X-ray measurements: The samples were placed in a dark faraday box with 70 μ m Aluminum window for X-ray irradiation. The radiation source is a Molybdenum tube X-ray broad spectrum with accelerating voltage of 35 kV (PANalytical PW2285/20) and Be window. The dose rate is variable in the range 10 – 70 mGy s⁻¹ on X-ray spot of 9 mm of diameter. A mechanical shutter controls the beam switching for 30s on and 30s off. The dose rates were previously calibrated employing the “Barracuda” dosimeter (RTI Group). Electrical measurements were acquired with Keithley SMU 2614.

Supporting Information

Supporting Information is available from the Wiley Online Library or from the author.

6. Acknowledgements

JEA thanks the US National Science Foundation (DMREF-1627428) for support of organic semiconductor development.

Received: ((will be filled in by the editorial staff))

Revised: ((will be filled in by the editorial staff))

Published online: ((will be filled in by the editorial staff))

References

- [1] B. D. Milbrath, A. J. Peurrung, M. Bliss, W. J. Weber, *J. Mater. Res.* **2008**, *23*, 2561.
- [2] S. Kasap, J. B. Frey, G. Belev, O. Tousignant, H. Mani, J. Greenspan, L. Laperriere, O. Bubon, A. Reznik, G. DeCrescenzo, K. S. Karim, J. A. Rowlands, *Sensors* **2011**, *11*, 5112.
- [3] A. Owens, A. Peacock, *Nucl. Instrum. Methods Phys. Res. Sect. Accel. Spectrometers Detect. Assoc. Equip.* **2004**, *531*, 18.
- [4] T. Takahashi, S. Watanabe, *IEEE Trans. Nucl. Sci.* **2001**, *48*, 950.
- [5] C. D. Dimitrakopoulos, P. R. L. Malenfant, *Adv. Mater.* **2002**, *14*, 99.
- [6] K. Fukuda, T. Someya, *Adv. Mater.* **2016**, n/a.
- [7] M. Kaltenbrunner, M. S. White, E. D. Glowacki, T. Sekitani, T. Someya, N. S. Sariciftci, S. Bauer, *Nat. Commun.* **2012**, *3*, 770.
- [8] Y. Li, G. Xu, C. Cui, Y. Li, *Adv. Energy Mater.* **2018**, *8*, 1701791.
- [9] B. Fraboni, A. Fraleoni-Morgera, N. Zaitseva, *Adv. Funct. Mater.* **2015**, n/a.
- [10] A. Ciavatti, E. Capria, A. Fraleoni-Morgera, G. Tromba, D. Dreossi, P. J. Sellin, P. Cosseddu, A. Bonfiglio, B. Fraboni, *Adv. Mater.* **2015**, *27*, 7213.
- [11] C. A. Mills, Y.-F. Chan, A. Intaniwet, M. Shkunov, A. Nisbet, J. L. Keddie, P. J. Sellin, *Phys. Med. Biol.* **2013**, *58*, 4471.
- [12] L. Basiricò, A. Ciavatti, T. Cramer, P. Cosseddu, A. Bonfiglio, B. Fraboni, *Nat. Commun.* **2016**, *7*, 13063.
- [13] S. Lai, P. Cosseddu, L. Basiricò, A. Ciavatti, B. Fraboni, A. Bonfiglio, *Adv. Electron. Mater.* **2017**, *3*, 1600409.

- [14] A. Ciavatti, T. Cramer, M. Carroli, L. Basiricò, R. Fuhrer, D. M. De Leeuw, B. Fraboni, *Appl. Phys. Lett.* **2017**, *111*, 183301.
- [15] H. M. Thirumanne, K. D. G. I. Jayawardena, A. J. Parnell, R. M. I. Bandara, A. Karalasingam, S. Pani, J. E. Huerdler, D. G. Lidzey, S. F. Tedde, A. Nisbet, C. A. Mills, S. R. P. Silva, *Nat. Commun.* **2018**, *9*, 2926.
- [16] H. Han, S. Lee, J. Seo, C. Mahata, S. H. Cho, A.-R. Han, K.-S. Hong, J.-H. Park, M.-J. Soh, C. Park, T. Lee, *Nanoscale Res. Lett.* **2014**, *9*, 610.
- [17] P. Büchele, M. Richter, S. F. Tedde, G. J. Matt, G. N. Anka, R. Fischer, M. Biele, W. Metzger, S. Lilliu, O. Bikondoa, J. E. Macdonald, C. J. Brabec, T. Kraus, U. Lemmer, O. Schmidt, *Nat. Photonics* **2015**, *9*, 843.
- [18] A. Intaniwet, C. A. Mills, M. Shkunov, H. Thiem, J. L. Keddie, P. J. Sellin, *J. Appl. Phys.* **2009**, *106*, 064513.
- [19] B. Fraboni, A. Ciavatti, F. Merlo, L. Pasquini, A. Cavallini, A. Quaranta, A. Bonfiglio, A. Fraleoni-Morgera, *Adv. Mater.* **2012**, *24*, 2289.
- [20] S. Yakunin, M. Sytnyk, D. Kriegner, S. Shrestha, M. Richter, G. J. Matt, H. Azimi, C. J. Brabec, J. Stangl, M. V. Kovalenko, W. Heiss, *Nat. Photonics* **2015**, *9*, 444.
- [21] Y. C. Kim, K. H. Kim, D.-Y. Son, D.-N. Jeong, J.-Y. Seo, Y. S. Choi, I. T. Han, S. Y. Lee, N.-G. Park, *Nature* **2017**, *550*, 87.
- [22] H. Zhang, Y. Yao, M. M. Payne, J. E. Anthony, J. W. Brill, *Appl. Phys. Lett.* **2014**, *105*, 073302.
- [23] R. J. Davis, M. T. Lloyd, S. R. Ferreira, M. J. Bruzek, S. E. Watkins, L. Lindell, P. Sehati, M. Fahlman, J. E. Anthony, J. W. P. Hsu, *J. Mater. Chem.* **2011**, *21*, 1721.
- [24] L. Basiricò, A. F. Basile, P. Cosseddu, S. Gerardin, T. Cramer, M. Bagatin, A. Ciavatti, A. Paccagnella, A. Bonfiglio, B. Fraboni, *ACS Appl. Mater. Interfaces* **2017**.
- [25] J. Tauc, R. Grigorovici, A. Vancu, *Phys. Status Solidi B* **1966**, *15*, 627.
- [26] R. H. Bube, *Photoconductivity of solids*; Wiley, 1960.
- [27] V. Raghuwanshi, D. Bharti, S. P. Tiwari, *Org. Electron.* **2016**, *31*, 177.
- [28] T. Cramer, L. Travaglini, S. Lai, L. Patruno, S. de Miranda, A. Bonfiglio, P. Cosseddu, B. Fraboni, *Sci. Rep.* **2016**, *6*, 38203.
- [29] S. Lai, I. Temiño, T. Cramer, F. G. del Pozo, B. Fraboni, P. Cosseddu, A. Bonfiglio, M. Mas-Torrent, *Adv. Electron. Mater.* **2018**, *4*, 1700271.

- [30] M. Kabir, S. Kasap, J. Rowlands, In *Springer Handbook of Electronic and Photonic Materials*; Prof, S. K.; Dr, P. C., Eds.; Springer US, 2007; pp. 1121–1137.
- [31] D. R. Shearer, M. Bopaiah, *Health Phys.* **2000**, *79*, S20.
- [32] I. Clairand, J.-M. Bordy, E. Carinou, J. Daures, J. Debroas, M. Denozière, L. Donadille, M. Ginjaume, C. Itié, C. Koukorava, S. Krim, A.-L. Lebacq, P. Martin, L. Struelens, M. Sans-Merce, F. Vanhavere, *Radiat. Meas.* **2011**, *46*, 1252.
- [33] H. Wei, Y. Fang, P. Mulligan, W. Chuirazzi, H.-H. Fang, C. Wang, B. R. Ecker, Y. Gao, M. A. Loi, L. Cao, J. Huang, *Nat. Photonics* **2016**, *10*, 333.
- [34] Y. Mei, M. A. Loth, M. Payne, W. Zhang, J. Smith, C. S. Day, S. R. Parkin, M. Heeney, I. McCulloch, T. D. Anthopoulos, J. E. Anthony, O. D. Jurchescu, *Adv. Mater.* **2013**, *25*, 4352.
- [35] J. E. Anthony, J. S. Brooks, D. L. Eaton, S. R. Parkin, *J. Am. Chem. Soc.* **2001**, *123*, 9482.
- [36] S. Subramanian, S. K. Park, S. R. Parkin, V. Podzorov, T. N. Jackson, J. E. Anthony, *J. Am. Chem. Soc.* **2008**, *130*, 2706.
- [37] P. Cosseddu, S. Lai, M. Barbaro, A. Bonfiglio, *Appl. Phys. Lett.* **2012**, *100*, 093305.
- [38] NIST, X-ray Mass Attenuation Coefficients. <https://www.nist.gov/pml/x-ray-mass-attenuation-coefficients>

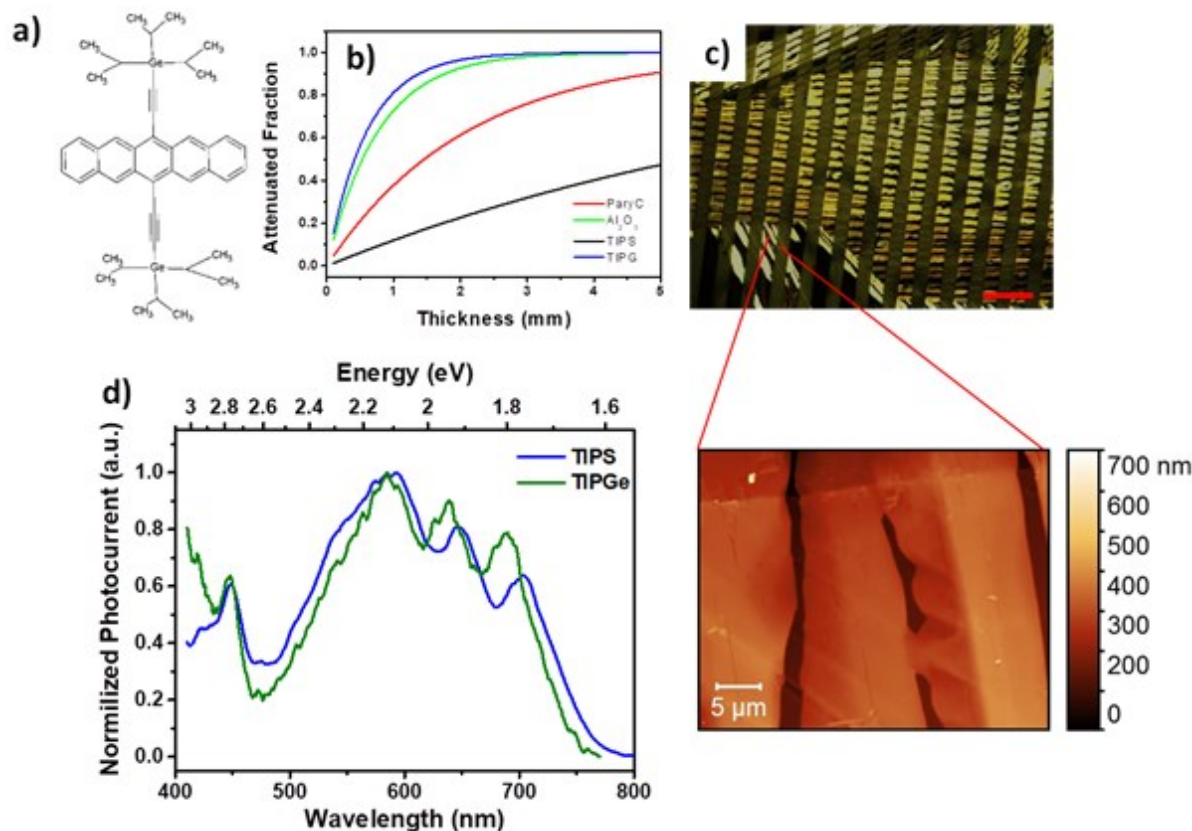


Figure 1. a) Chemical structure of the TIPGe-pentacene molecule. b) X-ray attenuated fraction at energy 17 keV as function of material thickness, showing the much smaller attenuation length of TIPGe compared to TIPS. The attenuated fraction in the thickness region of the final films is reported in **Figure S2**. c) Polarized-light optical microscope image of 200nm thick microcrystalline layer formed by drop cast a TIPGe 0.5%wt. solution in toluene onto plastic substrate. Red marker 100μm. Bottom: AFM image of a few crystallites. d) Photocurrent spectra of TIPS-pentacene (150nm thick, blue line) and TIPGe-pentacene (200nm thick, green line) thin films.

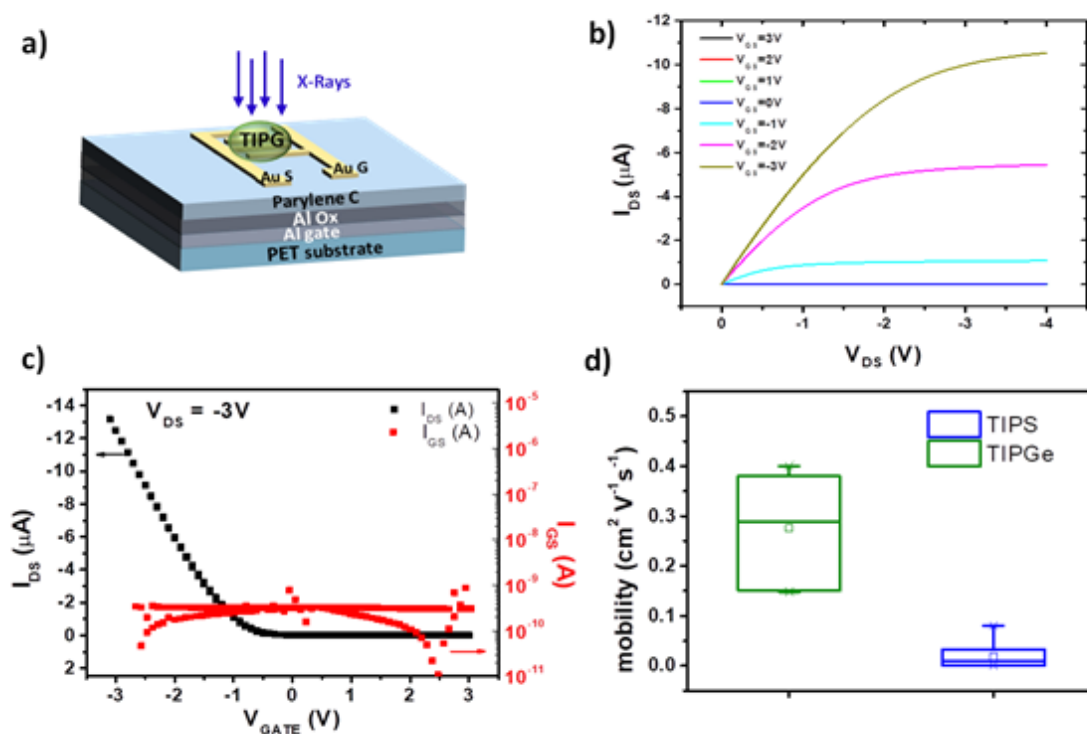


Figure 2. a) Schematic of the TIPGe-based X-ray detector. b) Typical output and c) transfer characteristic curves of low voltage transistors fabricated on plastic substrate based on TIPGe semiconductor. d) OTFT mobility comparison of TIPS and TIPGe on same PET flexible substrate.

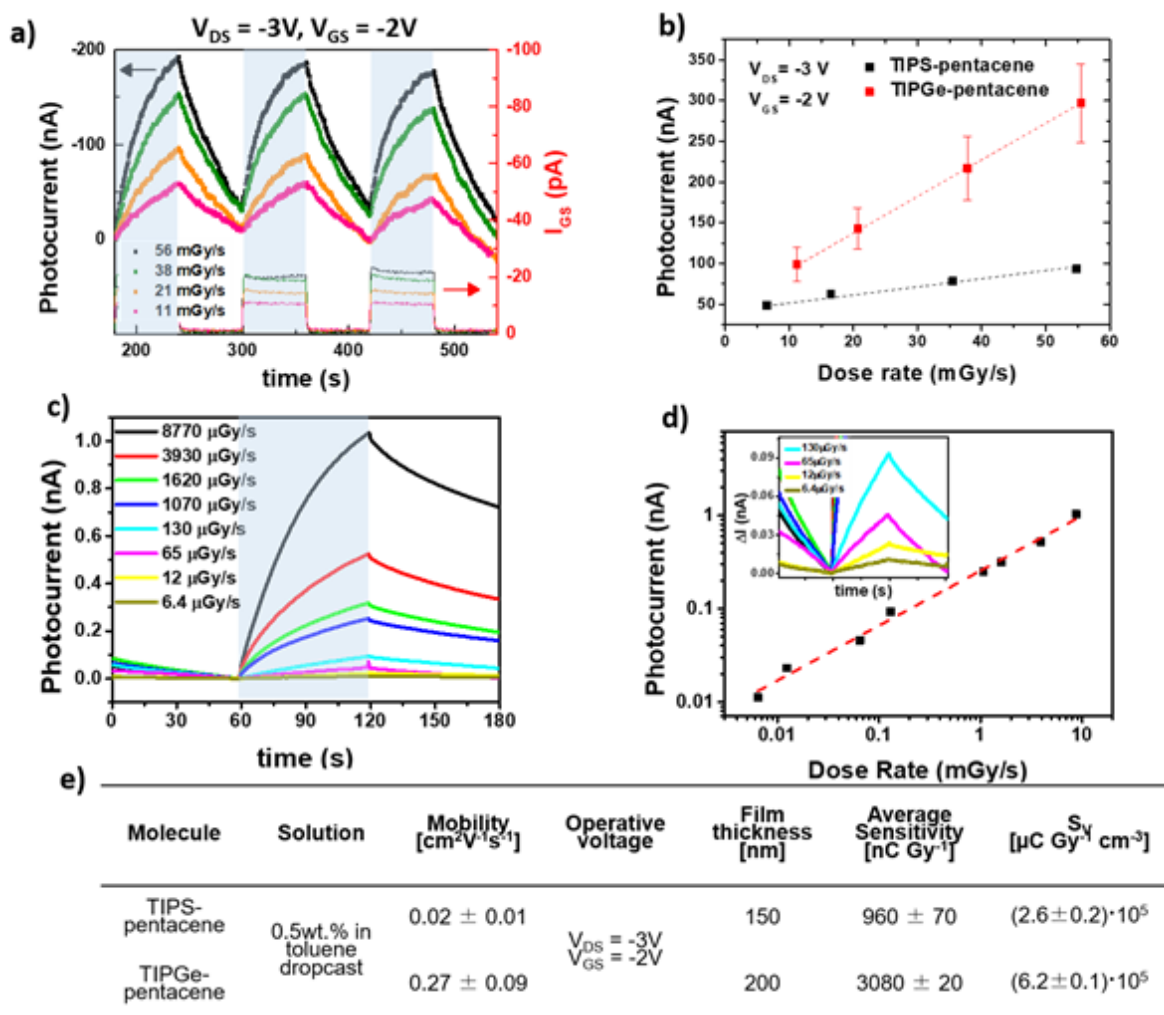


Figure 3. a) Typical Photocurrent signal (black arrow, left scale) and gate current (red arrow, right scale) of the TIPGe detector under ON/OFF X-ray irradiation at different dose rates. Blue shaded areas indicate X-ray ON, white areas indicate X-ray OFF. b) Comparison between X-rays induced photocurrent at different dose rates for TIPS (black squares) and TIPGe (red squares). c) Dynamic response of TIPGe at low dose rates, biased at $V_{DS} = -0.5V$ (linear region). d) X-ray induced photocurrent at very low dose rates, down to 6.4 $\mu\text{Gy/s}$. Inset: Corresponding photocurrent signal vs. time. e) Table with the comparison of mobility, sensitivity and sensitivity per unit volume values for TIPS- and TIPGe-based X-ray detectors.

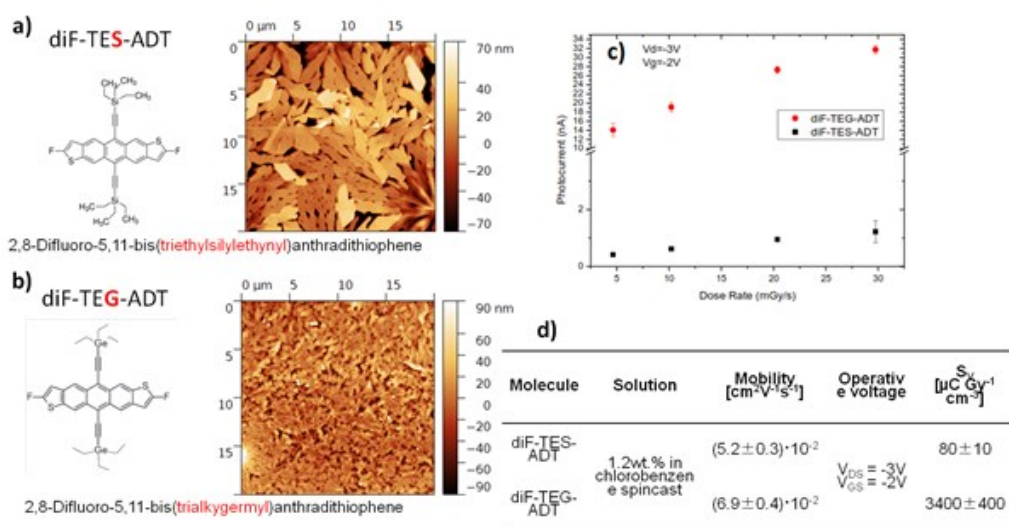


Figure 4. a) diF-TES-ADT and b) diF-TEG-ADT chemical structure and AFM morphology maps. c) Comparison between X-rays induced photocurrent at different dose rates for diF-TES-ADT (black squares) and diF-TEG-ADT (red circles). d) Table with the comparison of sensitivity unit volume values for diF-TEG-ADT and diF-TES-ADT-based detectors.

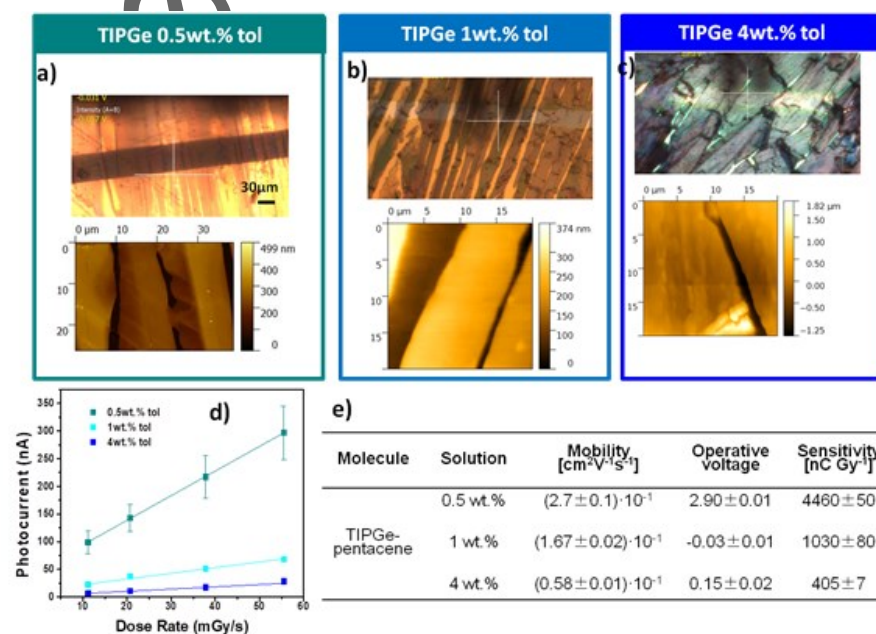


Figure 5. Role of organic molecule concentration on TIPGe drop-casted thin films in toluene solution: optical micrographs and AFM maps at 0.5wt.%(a), 1wt.%(b) and 4wt.%(c). Corresponding X-ray photocurrent (d) and summary of mobility, threshold voltage and X-ray sensitivity (e).

The X-ray detection performance of organic thin films on flexible plastic substrate have been boosted by chemical tailoring of new solution-processable organic molecules derived from TIPS-pentacene and diF-TES-ADT, with Ge-substitution in place of the Si atoms to increase the material atomic number.

Keyword: organic x-ray detectors, thin film transistors, tips-pentacene, tipge-pentacene

Andrea Ciavatti*, Laura Basiricò, Ilaria Fratelli, Stefano Lai, Piero Cosseddu, Annalisa Bonfiglio, John E. Anthony and Beatrice Fraboni*

Boosting direct X-ray detection in organic thin films by small molecules tailoring

ToC figure

